

# Evaluation of DCE-MRI data sampling, reconstruction and model fitting using digital brain phantom

Yinghua Zhu<sup>1</sup>, Yi Guo<sup>1</sup>, Sajan Goud Lingala<sup>1</sup>, Samuel Barnes<sup>2</sup>, R. Marc Lebel<sup>3</sup>, Meng Law<sup>1</sup>, and Krishna Nayak<sup>1</sup>

<sup>1</sup>University of Southern California, Los Angeles, CA, United States, <sup>2</sup>California Institute of Technology, Pasadena, CA, United States, <sup>3</sup>GE Healthcare, Calgary, Canada

**Target audience:** Researchers who develop dynamic contrast-enhanced (DCE) MRI techniques.

**Purpose:** Brain DCE MRI is a powerful technique for evaluating blood-brain-barrier leakage in tumors, multiple sclerosis lesions, and other neurologic disorders. DCE-MRI is an active area of research but lacks a gold standard making it difficult to evaluate novel image acquisition, reconstruction, and processing techniques. We introduce the use of patient-derived digital phantoms that provide ground truth and the ability to generate data with arbitrary temporal resolution, and perform sensitivity analysis over a broad range of inputs. We demonstrate its application to the evaluation of sparse sampling and constrained reconstruction methods.

## Methods & Results:

**Digital phantom:** Post-contrast whole-brain DCE-MRI data [1] from brain tumor patients were manually segmented into five non-overlapping regions: vessels, tumor boundary, tumor core, CSF, and other (see Fig. 1(a)).  $K^{\text{trans}}$  of tumor boundary and tumor core were 0.05 and 0.008  $\text{min}^{-1}$ , respectively (Fig. 1(b) bottom), which mimicked in-vivo estimates (Fig. 1(b) top). We added slight spatial smooth variation, and additional perturbations are possible to improve realism. PK parameters  $v_p$  and  $v_e$ , and tissue  $T_1$  for each region were given literature values [2,3]. A population-based arterial input function (AIF) [4], a two-compartment exchange model [2], and the steady state SPGR signal equation, were used to generate the time intensity curves (Fig 1(c)), which were used to fabricate dynamic images. We then applied measured coil sensitivities, took the Fourier transform, and added noise using the measured channel noise covariance. Coil sensitivity maps and noise covariance matrix were estimated from the in-vivo data. B1+ variation and T2\* decay were not modeled, but could be included later.

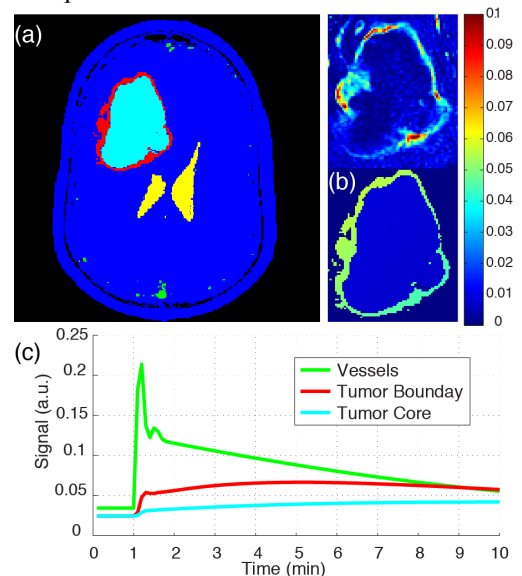


**Figure 1.** (a) Phantom segmentation; (b) Clinical (top) and phantom ground truth (bottom)  $K^{\text{trans}}$ ; (c) Time intensity curve of three main regions.

**Potential uses:** Brain DCE phantoms could allow us to address major questions like: What is optimal temporal resolution? How dependent are results on the timing and accuracy of the AIF? What is the impact of sparse sampling and constrained reconstruction? What techniques can be used to minimize bias and variance of estimated PK parameter maps?

**Example use:** For demonstration, we have used the phantom to explore the bias and variance of tumor  $K^{\text{trans}}$  maps when using sparse sampling and constrained reconstruction. We generated multiple replicas of the phantom using PD [1] and GLACIER [5] sampling at different acceleration rates. Images were reconstructed using temporal total variation, with empirically chosen regularization parameter. The AIFs for model fitting were derived from reconstructed vessel signals, and the  $K^{\text{trans}}$  was estimated using the Patlak model [6]. Fig. 2 shows the bias and standard deviation (STD) of tumor  $K^{\text{trans}}$  from reconstruction of multiple replicas of PD and GLACIER sampling at temporal resolution 7.9 sec and 3.9 sec, corresponding to reduction factor R of 50 and 100. The bias was calculated using the reference phantom tumor  $K^{\text{trans}}$ , and the STD was calculated from multiple replicas of fitted  $K^{\text{trans}}$ . PD sampling resulted in slightly lower and more uniform bias than GLACIER sampling; GLACIER resulted in lower STD than PD sampling. Generally, as R increased, bias increased likely due to loss of reconstructed image quality, and STD decreased likely because more time points were available for model fitting.

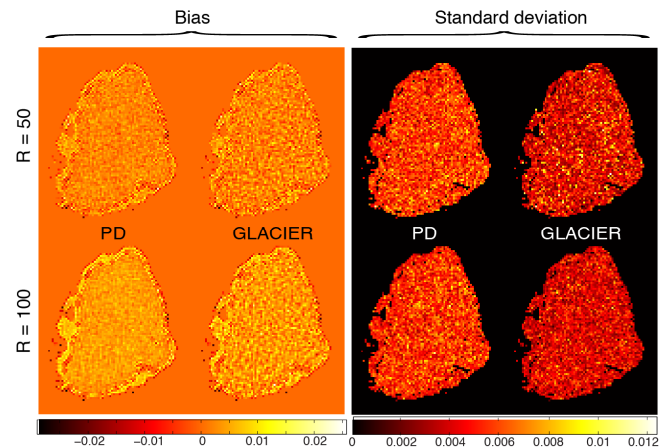


**Figure 2.** Bias and standard deviation of phantom tumor  $K^{\text{trans}}$  fitted from reconstruction of multiple replicas of PD and GLACIER undersampling at R of 50 and 100.

**Conclusion:** We have developed a 3D brain tumor phantom that can be used to evaluate novel DCE-MRI methods. We demonstrate its use for the evaluation of data sampling, image reconstruction, and PK parameter modeling. The phantom provides parameter ground truth and arbitrary temporal resolution that are not available from retrospective studies using in-vivo data.

**Reference:** [1] Lebel, *et al.* MRM 2014; [1] Sourbron, *et al.* MRM 2011; [3] Tofts, Signal 2010; [4] Parker, *et al.* MRM 2006; [5] Zhu, *et al.* ISMRM 2014 p4365; [6] Patlak, *et al.* JCBFM 1983.